Journal of Applied Polymer Science

Effects of raw and poly(propylene oxide) grafted nanosilica on the morphology and thermal and mechanical properties of polyurethane foam

Xia Gao,[1,2] Keping Chen,[1] Shuen Liang,[1] Chunchun Fan,[1,2] Yigang Huang,[1,2] Xiaorong Jia,[1] Chunrong Tian,[1,2] Jianhua Wang[1,2]

[1]Institute of Chemical Materials, China Academy of Engineering Physics, Mianyang 621900, Sichuan, China
[2]College of Materials Science and Engineering, Southwest University of Science and Technology, Mianyang 621010, Sichuan, China
Correspondence to: C. Tian (E-mail: tianchr1972@163.com) and J. Wang (E-mail: wjh@caep.ac.cn)

ABSTRACT: Poly(propylene oxide) (PPO)-grafted nanosilica (NS)/polyurethane foam (PUF) composites were synthesized by a ring-opening polymerization catalytic process and reaction-molding technology. The raw NS and PPO–NS were characterized by Fourier transform infrared spectroscopy, thermogravimetric analysis, and transmission electron microscopy. Scanning electron microscopy, dynamic mechanical analysis, and compressive strength tests were used to compare the morphology and thermal and mechanical properties of the PPO–NS/PUF and raw NS/PUF composites with a series of filler contents. The PPO–NS/PUF composites generally exhibited better morphology, thermal and mechanical properties than raw NS/PUF composites. Moreover, the PPO–NS/PUF composites with lower contents (0.5, 1 php) of filler showed even higher mechanical reinforcement than that with higher contents (1.5, 2 php) of filler, which was caused by the interaction between additives and PUF matrix. © 2015 Wiley Periodicals, Inc. J. Appl. Polym. Sci. **2015**, *132*, 42400.

KEYWORDS: composites; grafting; polyurethanes

Received 2 December 2014; accepted 21 April 2015
DOI: 10.1002/app.42400

INTRODUCTION

Polyurethane foam (PUF) has many advantages, including its easy processing, low density, high strength, high recoverable strain, and low manufacturing cost.[1] In the past several years, PUF has received increasing attention because of its excellent mechanical properties and heat resistance; these depend on the nature and amounts of polyether polyol, isocyanate, and chain extender.[2] However, it still has some limits in its shock resistance and heat-insulation performance compared with the polymer matrix.[3,4]

The reinforcement of PUF is usually achieved in PUF composites through the addition of reinforcing particles[5] into the polyurethane matrix, and many amazing results have recently been reported with nanofillers such as silica/PUF nanocomposites.[6–9] Ting *et al.*[10] reported that the addition of 1.4% fumed silica made the cell distribution more uniform in PUF, and the temperature of degradation occurring with the maximum weight loss rate was about 7°C higher than that of pure PUF. Javni *et al.*[11] studied the effect of nanosilica and microsilica fillers on the properties of PUF; they found that the nanofiller, as an additional physical crosslinker, increased the modulus of the flexible segment in the polyurethane matrix. This resulted in increased hardness and compressive strength. The microfiller in flexible foams lowered the hardness and compression strength but increased rebound resilience. Nunes *et al.*[12] found that the Young's modulus and hardness increased as the silica concentration increased, and although composites with silica bearing a

Xia Gao, Keping Chen, Chunrong Tian, and Jianhua Wang contributed to the conception and design of this article. Chunrong Tian and Jianhua Wang obtained financial support. Yigang Huang, Xiaorong Jia, Chunrong Tian, and Jianhua Wang contributed administrative support. Shuen Liang, Chunchun Fan, Yigang Huang, Xiaorong Jia, Chunrong Tian, and Jianhua Wang provided the study materials. Xia Gao, Keping Chen, Chunchun Fan, Chunrong Tian, and Jianhua Wang contributed to the collection and assembly of data. Xia Gao, Keping Chen, Shuen Liang, Chunchun Fan, and Chunrong Tian contributed to the data analysis and interpretation. Xia Gao, Keping Chen, Chunchun Fan, and Chunrong Tian wrote the article. All of the authors provided final approval of the article.

high occurrence of silanol groups presented quite large changes in the modulus and hardness, the final deformation was almost the same as that of the pure polymer. It has also been reported that shape memory of polyurethane–silica hybrids obtained from a thermomechanical test exhibited good shape retention and a shape recovery of more than 80% with the addition of 10 wt % tetraethoxysilane.[13]

However, nanosilica (NS) particles tend to be aggregates in common solvents and have a weak interfacial interaction with the polymer matrix,[5,11,13,14] so chemical modification of NS particles is greatly needed to improve the performance of PUFs.

Several approaches, including a coupling agent process,[15] esterification,[16] and polymer grafting,[17] have been introduced to overcome these problems. Among these approaches, polymer grafting is very effective because of its controllable molecular weight, ordered molecular structure, and strong chemical bonding between the polymer matrix and NS. Another significant advantage of this process is that the polymer chains are covalently attached to the surface. In addition, a large variety of initiating mechanisms, including free-radical polymerization,[18] living anionic polymerization,[19] atom transfer radical polymerization,[20] reversible addition fragmentation chain-transfer polymerization,[21] click polymerization,[20] ring-opening polymerization (ROP),[22,23] and direct attachment with a functional polymer,[24] can be used. Generally, polymerization starts from the functional groups, such as —OH on the surface of NS, which are derived from some of the siloxane groups (Si—O—Si). Joubert *et al.*[22] synthesized poly(ethylene oxide)-grafted silica nanoparticles with a silica core and a hairy poly (ethylene oxide) layer with a controlled heterogeneous ROP catalytic process. Khan and Huck[19] demonstrated a procedure to synthesize covalently linked hyperbranched polyglycidol brushes on Si/SiO_2 surfaces via the anionic ring-opening multibranching polymerization of glycidol at 110°C. On the basis of the previous results, the grafting polymer generally had some groups, such as C—O—C groups; this was the same with polyether polyol, which is the key ingredient in the preparation of PUF. Moreover, the same groups in the grafting polymer and polymer matrix would result in a better dispersion and mechanical reinforcement, as confirmed by rheological analysis.[16,21] Therefore, PUF with poly(propylene oxide) (PPO)-grafted NS is worth studying because there are the same groups between the PPO and polyether polyol, and the mechanical reinforcement has so far been shown with the addition of bare NS.[6–8,25]

In this study, PPO–NS was prepared successfully with an ROP catalytic process, and NS/PUF composites were synthesized. The different effects of NS and PPO–NS on the morphology and thermal and mechanical properties of PUF, respectively, were investigated.

EXPERIMENTAL

Materials

Tetraethyl silicate was supplied by Sinopharm Chemical Reagent Co., Ltd., and was used as received. 3-Glycidoxypropyl trimethoxysilane (GPS; >99.7%, Aladdin) was used as received. Aluminum isopropoxide [$Al(O^iPr)_3$; >99.99%, Aladdin] was dissolved in toluene (0.025*M*) and stored over molecular sieves (4 Å, Kermel). Sodium [analytical reagent (AR)] was purchased from Tianjin Kermel Chemical Reagent Co., Ltd. Propylene oxide (AR) was purchased from Chengdu Kelong Chemical Reagent Factory and was used as received. Absolute ethanol (>99.7%), ammonia solution (AR) and toluene (>99.5%) were supplied by Chengdu Institute of Chemical Reagents Joint. Moreover, toluene was distilled from sodium.

Polyether polyol (model N303, OH value = 458.2 mg of KOH/g) was obtained from Jiangsu Jinqi Polyurethane Co., Ltd. Polyaryl polymethylene isocyanate (PAPI; NCO content = 31.2 wt %) was purchased from WANNATE Chemical Group Co., Ltd. Silicone glycol copolymer (AK8807, Jiangsu Maysta Chemie AG) was used as a surfactant, and triethanolamine [AR, Chongqing Chuandong Chemical (Group) Co., Ltd.] was used as the catalyst. Distilled water was used as a blowing agent in this study.

Preparation of the PPO-Grafted NS

Synthesis of NS Particles.[26] Tetraethyl orthosilicate (124.88 g) and anhydrous ethanol (100 mL) were introduced into a reaction flask containing a solution of absolute ethanol (900 mL), distilled water (72.00 g), and ammonia water (25.97 g), which had been stirred for 20 min at room temperature. The mixture was stirred continuously for 3 h, centrifuged repeatedly (10,000 rpm for 10 min), and then dispersed into water to remove the unnecessary solvent. The products were then dried *in vacuo* at 100°C for 2 days. The resulting NS particles were defined as raw NS.

Covalent Attachment of GPS onto the NS Surface.[23] About 25 mL of GPS was dissolved in 250 mL of a pH 2.0 sulfuric acid solution. The prehydrolyzed GPS solution was heated to 100°C in an oil bath for 1 h and introduced into a flask containing 7.5 g of silica. The mixture was stirred magnetically at 100°C for 4 h. The grafted silica beads were centrifuged repeatedly (10,000 rpm for 20 min) and dispersed into water to remove the nonreacted silane. The products were then dried *in vacuo* at 140°C for 3 h, and the resulting NS particles were defined as GPS–NS.

Graft Polymerizations. All of the polymerizations were performed in an autoclave. After the addition of $Al(O^iPr)_3$ to the GPS–NS dispersion in toluene, the solution was protected under dry nitrogen. Then, the mixture was heated to 80°C after the addition of the PO monomers.[22]

After 1 day, a mixture of ethanol and distilled water was added to remove the free nongrafted polymer chains from the suspension medium by successive centrifugation (10,000 rpm for 20 min)–redispersion cycles. The products were further extracted in a Soxhlet extractor with ethanol for 4 h to remove the ungrafted polymer. The polymer-grafted NS particles were then dried *in vacuo* at 50°C for 10 h, and the resulting particle was defined as PPO–NS.

The preparation process of PPO–NS is schematically illustrated in Figure 1. Two main steps were taken to obtain PPO–NS. First, NS particles were modified with GPS to produce GPS–NS. Then, the grafting of PPO onto GPS–NS was performed

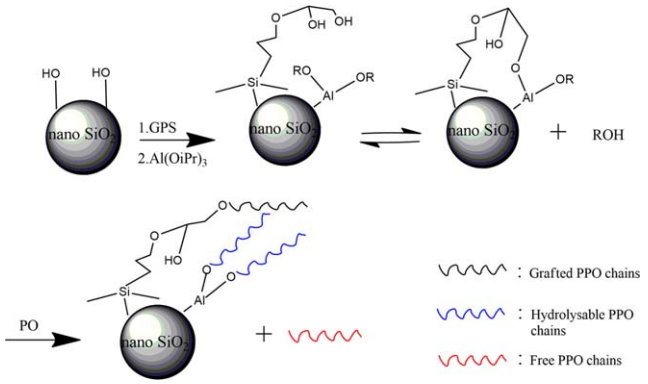

Figure 1. Schematic illustration of the grafting process of PPO on the surface of NS. [Color figure can be viewed in the online issue, which is available at wileyonlinelibrary.com.]

through a ROP process. During the process, the polymerization of propylene oxide was initiated from the surface of GPS–NS with $Al(O^iPr)_3$ as the initiator and catalyst. Additionally, the GPS–NS played the role of co-initiator and chain-transfer agent in the polymerization; this enabled the formation of irreversibly bonded polymer chains. The obtained products were washed by successive centrifugation (10,000 rpm for 20 min)–redispersion cycles in a water–ethanol mixed solvent and extracted in a Soxhlet extractor with ethanol as the medium to remove ungrafted polymer. The products were analyzed by Fourier transform infrared (FTIR), thermogravimetric analysis (TGA), and transmission electron microscopy (TEM).

Preparation of the Rigid PUF

The rigid PUF sample was prepared by the mixture of both polyether polyol N303 and PAPI at 25°C with a mechanical stirrer. First of all, distilled water, the catalysts, and the surfactant were added to the polyol solution. Then, stirring was begun from a speed of 100 rpm, and the speed was gradually increased to 2000 rpm within 5 min after the NS particles were added to the polyol solution. The amounts of NS added were 0.5, 1.0, 1.5, and 2.0 php, respectively. After that, PAPI was added to the polyol mixture prepared by the process mentioned previously at a rotation speed of 2000 rpm for 2 min at room temperature. Finally, the mixture was immediately poured into an aluminum mold for the molded foaming process; it was kept at room temperature for 3 h. The foam was then cured with the mold at 100°C in an oven for 3–4 h before characterization.

Characterization

FTIR Spectroscopy. The FTIR spectra of NS were recorded between 400 and 4000 cm^{-1} on a Nicolet 6700 FTIR spectrometer with KBr pellets before analysis.

TGA. The amount of the grafted polymer was studied by TGA with an SDT 2050 apparatus from TA Instruments under a stream of nitrogen with the temperature increasing at 20°C/min from 50 to 800°C. Moreover, a constant temperature of 100°C for 5 min was applied before each measurement to remove the water absorbed on the surface of the samples.

TEM. TEM was used to investigate the microstructure on the surface of NS. For the TEM experiments, one drop of the diluted dispersion of ethanol was spread onto a carbon film supported by a calibrated copper grid and allowed to dry in air before analysis. The TEM instrument used was a Zeiss Libra 200 FE (Germany); an acceleration voltage of 200 kV was applied.

Scanning Electron Microscopy (SEM). The morphology of the PUF was observed on a CamScan Apollo 300 field emission scanning electron microscope with an accelerating voltage of 10 kV. For the SEM experiments, the samples were fixed on an aluminum disc with a conductive adhesive, and the surfaces were coated with Au–Pd under argon with an electric current of 25 mA for 2 min to ensure a good conductivity of the samples. Image-Pro Plus software was used here to calculate the size distribution of the cellular structure.

Dynamic Mechanical Analysis (DMA). DMA was carried out with an RSA-III solid rheometer from TA Instruments at a heating rate of 3°C/min from room temperature to 180°C. The dimensions of the samples were 45 × 12 × 2 mm^3 at a fixed frequency of 1 Hz with a strain of 0.1%.

Compressive Test. The compressive strength of the PUF samples with dimensions of 2 × 20 × 20 mm^3 were measured with an Instron 5500 universal testing machine according to GB/T 8813-2008. The crosshead speed of the compression was set at 5 mm/min. The value of the compressive strength was recorded when the samples reached 10% deformation. Four groups of data for each material were obtained, and an average value from three of their close data values was used.

RESULTS AND DISCUSSION

Formation of PPO on the Surface of NS

FTIR Analysis of NS and PPO–NS. There were three kinds of polymer chains formed at the end of the polymerization process: free nongrafted PPO chains initiated by the alcohol groups released during the grafting of $Al(O^iPr)_3$, weakly bonded hydrolyzable PPO chains attached to the silica surface by means of aluminum alkoxide, and hydrolytically stable grafted PPO

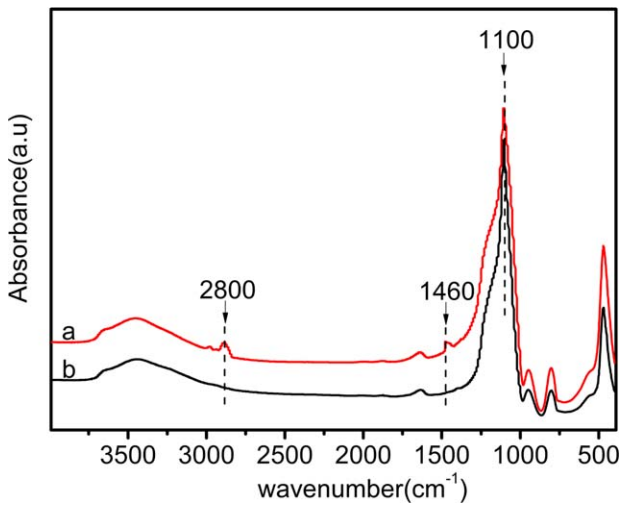

Figure 2. FTIR spectra of (a) PPO–NS and (b) GPS–NS. [Color figure can be viewed in the online issue, which is available at wileyonlinelibrary.com.]

Table I. Graft Polymerization of PPO on the Surface of NS Particles

TGA (wt %)[a]	Grafted amount (g/g of silica)[b]	Grafting efficiency (%)[c]	Conversion (%)[d]
10	0.11	6.4	21.4

[a] Weight loss between 50 and 800°C.
[b] Calculated with eq. (1).
[c] Determined with the following equation:
Grafting efficiency (%) = (Surface polymer/Total polymer formed) × 100
[d] Determined by pressure measurements after 1 day of reaction.

chains initiated by the grafted alcohol molecules. After selective separation of the free and hydrolyzable PPO by alcoholysis and extensive washing by a series of centrifugation–redispersion cycles in distilled water and extraction in a Soxhlet extractor with ethanol as the medium, NS particles containing the grafted PPO chains were isolated and characterized. The presence of PPO–NS was qualitatively evidenced by FTIR spectroscopy, as shown in Figure 2, which shows characteristic signals of both silica ($\nu_{Si—O—Si}$ at 1100 cm $^{-1}$) and PPO (ν_{CH2} at 2800 cm^{-1} and δ_{CH2} at 1460 cm^{-1}). These confirmed the grafting of PPO on the surface of NS.

TGA of NS and PPO–NS. The results are reported in Table I for the polymerization of PPO on the surface of NS. The weight loss determined by TGA is shown in Figure 3. For GPS–NS, there was only a very slight decomposition peak around 500°C and a weak decomposition peak before 110°C; this was related to the silane and absorbed water on the NS. After grafting, a thermal decomposition peak appeared between 247 and 403°C; this was attributed to the grafted polymer part. It was found that the total weight loss was about 13.6%, and the weight loss of silane and water was around 4%. Thus, about 10% PPO was grafted on the surface of NS; this corresponded to the grafted amount of 0.11 g/g of silica, with the assumption that the PPO was grafted effectively on the surface of NS by means of the ROP catalytic process. The conversion of 21.4% was rather low, and the NS displayed a catalytic activity because they contained a certain amount of active species. Moreover, the amount of active species was a determinant of the fraction of covalently bonded polymer chains, which corresponded to the grafting efficiency of 6.4%.[22]

TEM Analysis of NS and PPO–NS. The morphology of the grafted PPO on NS was observed by TEM. TEM images of the bare NS and PPO–NS are shown in Figure 4. Figure 5 shows the particle size distribution calculated from the TEM observation. As presented in Figure 5, the bare NS particle size varied from 65 to 185 nm and presents a narrow size distribution. The average diameter of the NS was about 128 nm. The PPO–NS particle size ranged from 86 to 183 nm, and it also presented a narrow size distribution with an average diameter of 135 nm. Figure 4(a) shows spherical silica beads with a smooth edge and a mean diameter of around 128 nm. What is more interesting was the TEM picture after grafting [Figure 4(b)]; this clearly shows gray zones of low-density filling the space between the silica spheres and a rough edge around each silica particle; this could be attributed to the PPO formed on the silica surface. A certain thickness of the PPO layer around each silica particle was observed directly from the TEM picture; this indicated that there was a dense polymer shell formed on the surface of NS. The diameter of the resulting core–shell particles ($Dp_{core–shell}$) was calculated according to eq. (2):

$$Dp_{core\text{-}shell} = Dp_{Sio2}\sqrt[3]{\left(1+\text{Grafted amount}\times\frac{\rho_{Sio2}}{\rho_{PPO}}\right)} \quad (2)$$

where Dp_{SiO2} is the diameter of the silica particles before grafting; ρ_{SiO2} and ρ_{PPO} are the densities of the SiO_2 and PPO, respectively; and the grafted amount is the polymer content (g/g of silica), as reported in Table I. According to data available on the Internet, ρ_{SiO2} and ρ_{PPO} are 2.2 g/cm^3 and 1.01 g/mL, respectively. Thus, Dp_{SiO2} was determined by eq. (2) to be around 135.68 nm; this corresponded to a shell thickness of 3.8 nm. These values were in close agreement with the TEM observations. Consequently, it was clear that the PPO was grafted effectively on the surface of NS. However, the grafted polymer layer around the NS particles was thin and irregular because of the irregular chain growth during the polymerization process.

Morphology and Mechanical Properties of the NS/PUF Composites

As shown in the results of recent investigations, nanoparticles effectively reduce the cell size of PUF during the foaming process.[27–29] The dispersion of nanoparticles in the polymer matrix is a well-known challenge and is due to the entangled agglomerates that result from the intrinsically strong interactions of nanoparticles adjoining with each other.[30,31] Moreover, the porous structure of polymer foams limits the distribution of fillers in the cell walls and cell struts to form effective reinforcing networks.[32–34] In the literature, several processing techniques have been introduced extensively to improve the thermal insulation and mechanical properties of PUF by reducing cell size and improving the uniformity of the morphology in the PUF.[32,35–44]

The ultrasonically assisted NS dispersion in polyether polyol was optimized in this study. Figure 6 shows the typical cellular structure of the NS/PUF and PPO–NS/PUF composites with different contents (0, 0.5, 1, 1.5, and 2 php) of fillers. With increasing filler contents (0, 0.5, and 1 php), the average cell

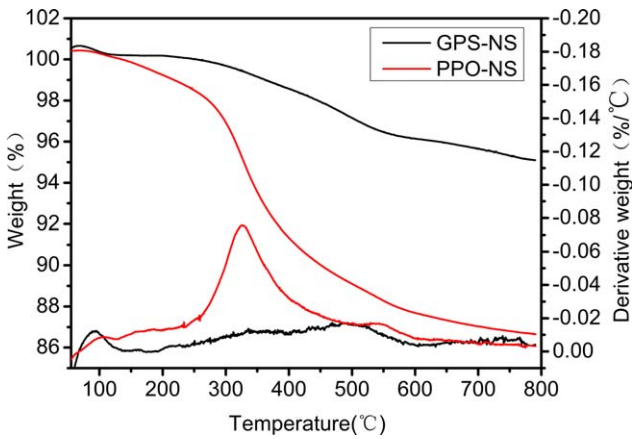

Figure 3. TGA images of GPS–NS and PPO–NS. [Color figure can be viewed in the online issue, which is available at wileyonlinelibrary.com.]

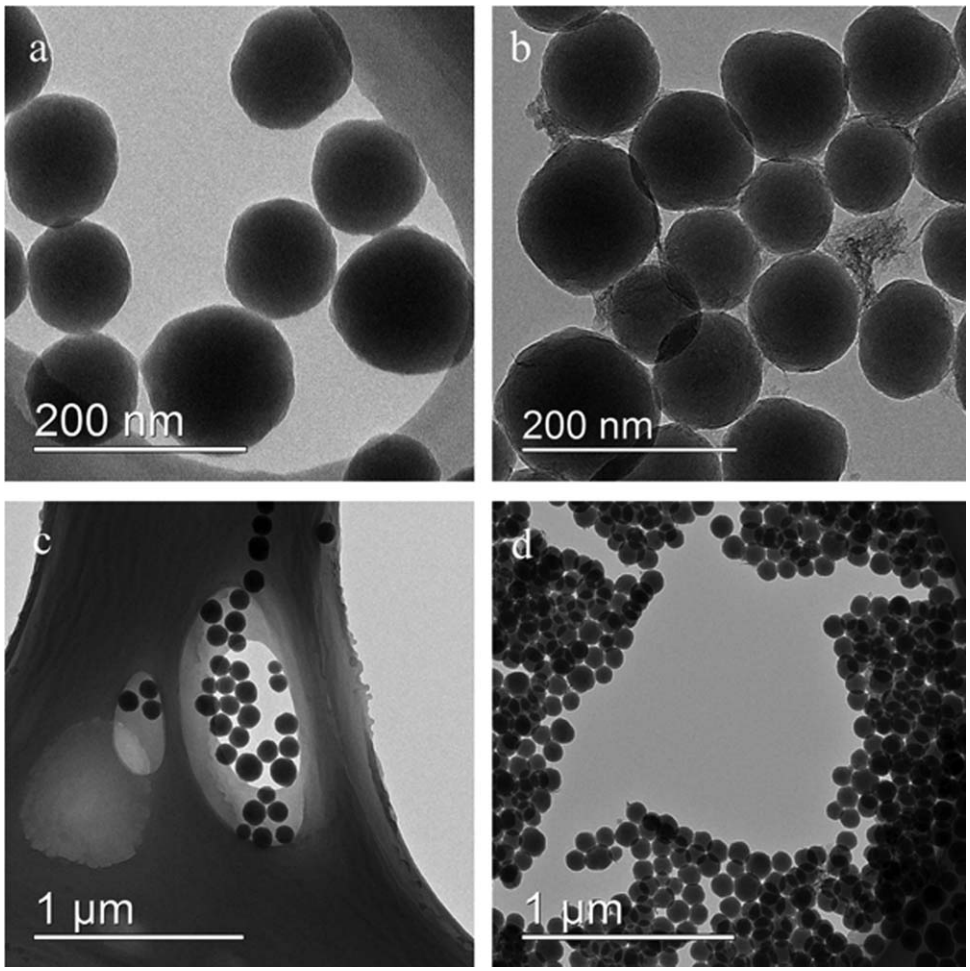

Figure 4. TEM images of the (a,c) raw NS and (b,d) PPO–NS.

size decreased gradually; this indicated that NS could serve well as a heterogeneous nucleating agent during the foaming process. However, the average cell size of the composites with contents of 1.5 and 2 php displayed a slight increase, and some ruptures occurred in the bubbles because the redundant additives acted as overfull heterogeneous nucleating agents; they crowded and coalesced the bubbles to produce bigger or breaking ones. Correspondingly, the average cell size of the PPO–NS/PUF composites with different filler contents changed in a similar regularity with that of the NS/PUF composite.

As presented in Figure 7, compared to the cell size of NS/PUF, the cell size with the addition of PPO–NS with the same content decreased, and this generated an apparent reduction in the rupture and inhomogeneity. These results indicate that PPO–NS had a significant heterogeneous nucleation effect on the foaming process compared to that of common NS particles for PUF.[44] With specific surface structure and strong interfacial interaction, PPO–NS should be more valid than NS for reducing the nucleation free energy and creating effective nucleation sites.[31,44]

DMA of the NS/PUF Composites

The damping performance of PUF, generally known as the dynamic properties, which is of great significance in packaging materials, can be characterized by DMA.

In the glass-transition region, the energy dissipation increases greatly, and the loss factor (tan δ) reaches a maximum. The glass-transition temperature (T_g) is associated with the α

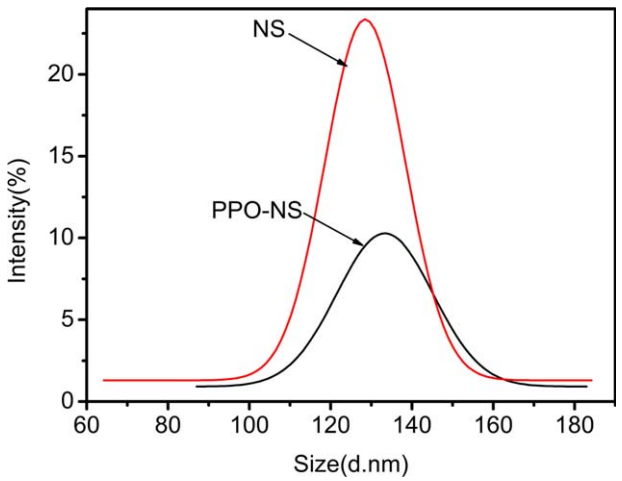

Figure 5. Particle size distributions of the raw NS and PPO–NS. [Color figure can be viewed in the online issue, which is available at wileyonlinelibrary.com.]

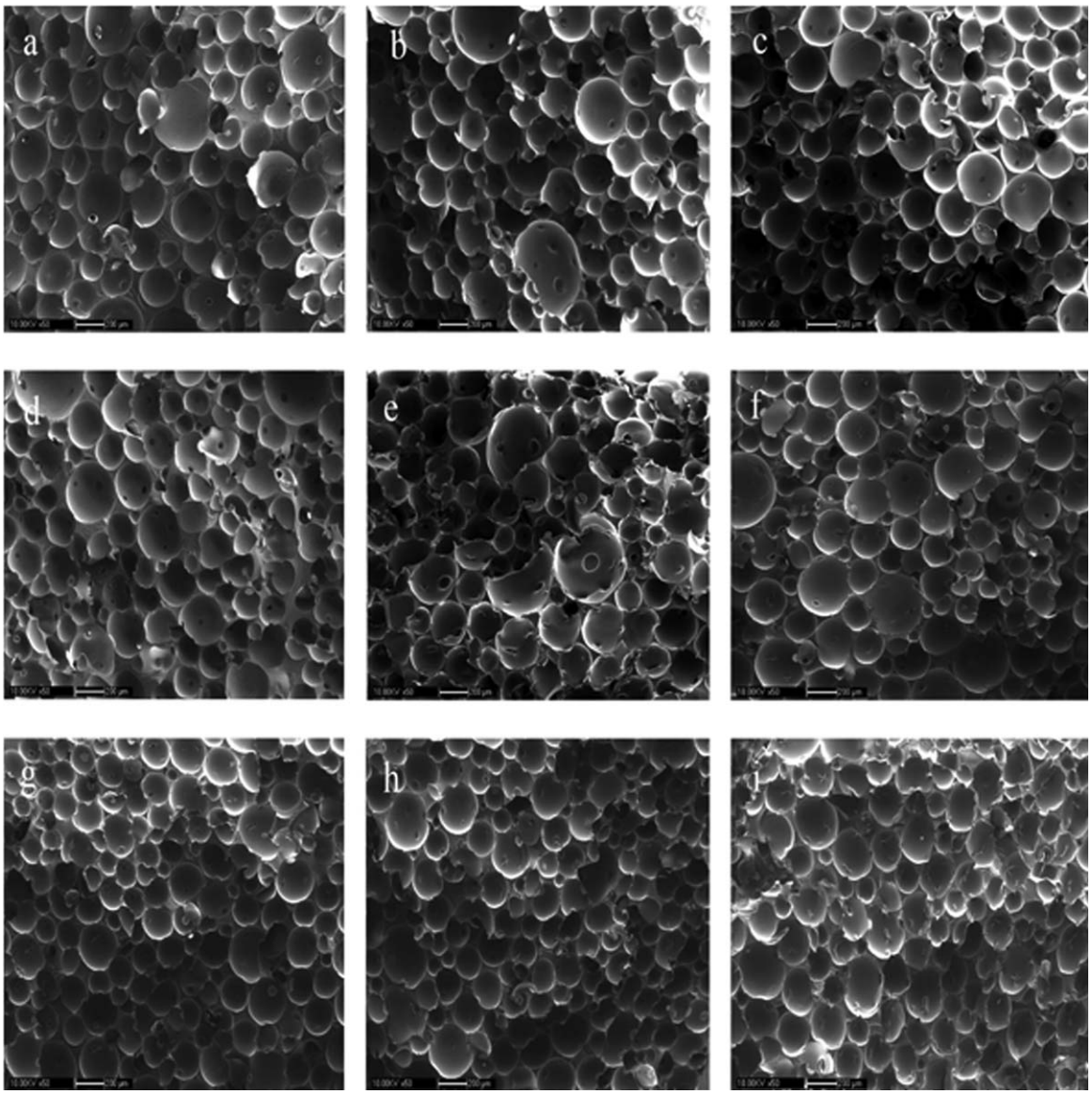

Figure 6. SEM morphologies and bubble size distributions of PUFs with different NS contents [(a) pure PUF and (b) 0.5, (c) 1, (d) 1.5, and (e) 2 php] and different PPO–NS contents [(f) 0.5, (g) 1, (h) 1.5, and (i) 2 php].

relaxation of the mobility and movement capacity of polymer chain segments in PUF composites.[39]

As presented in Figure 8, the apparent T_g values of the PUFs filled with 0, 0.5, 1, 1.5, and 2 php of NS were 125, 131, 133, 134, and 136°C, respectively. We found that the T_g values and the temperature range for the damping effect of all of the filled PUF composites were improved with increasing amount of NS; this demonstrated the stiffening barrier effect of NS, which impeded the polymer chain motion via strong interfacial interactions and acted as a physical crosslink during the glass transition.[45] It is noteworthy that the apparent T_g of PUF filled with 0.5, 1, 1.5, and 2 php of PPO–NS were 134, 136, 130, 129°C, respectively. Undoubtedly, the PPO–NS loading induced a greater increase in T_g with lower contents (0.5 and 1 php) of filler compared to NS. However, the PPO–NS/PUF composites loaded with higher contents (1.5, 2 php) of filler exhibited a lower T_g than those with lower contents (0.5 and 1 php) of filler. This was attributed to the strong interaction between the grafted polymer and matrix, together with a steric stabilization effect of the grafted polymer. The grafted polymer formed a barrier and reduced the attractive forces between NS particles through a well-known entropic stabilization mechanism.[3] For dispersion and mechanical reinforcement, the amount of grafting polymer and polymer-grafted NS were key factors. A high quantity of polymer-grafted NS led to particle coagulation because of their numerous chain bridge effects because the same groups also existed among themselves; this could change the particle dispersion state and resulted in a nonuniform cell size distribution and lower T_g. The polymer-grafted NS with a medium quantity was easier to blend with free polymer chains than a high quantity and provided a better dispersion and steric stabilization effect in the polymer matrix.

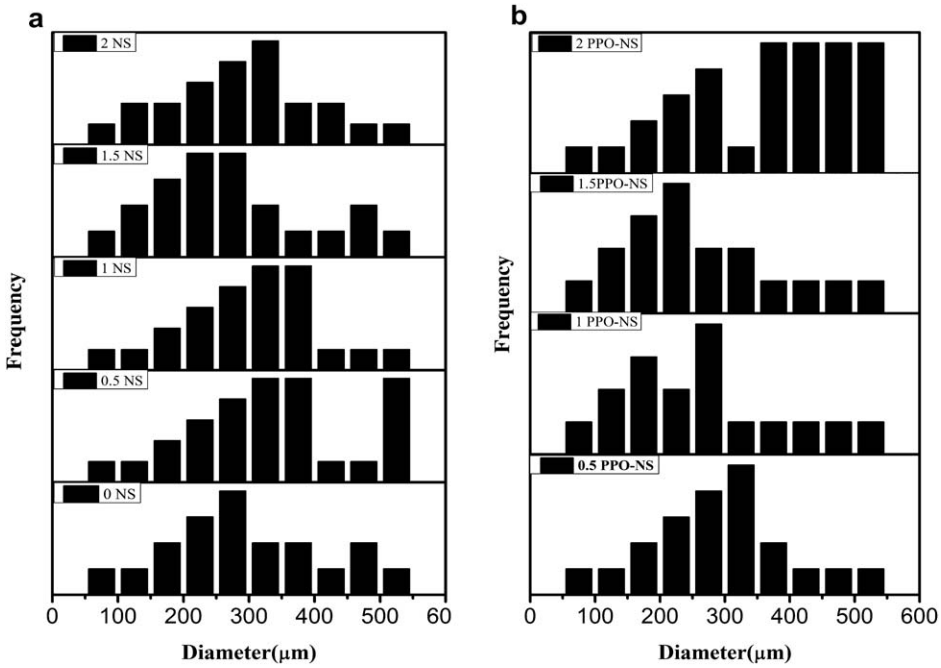

Figure 7. Bubble size distributions of PUFs with (a) different NS contents (0, 0.5, 1, 1.5, and 2 php) and (b) different PPO–NS contents (0.5, 1, 1.5, and 2 php).

As presented in Figure 9, the incorporation of increasing contents (0, 0.5, 1, 1.5, and 2 php) of NS induced a general rise in the storage modulus (E'; 29.3, 59.5, 70.1, 85.1, and 73.3 MPa) of the NS/PUF composites at room temperature. The observed enhancement in the mechanical response was attributed to the effective load transfer from the PU matrix to the high-strength, homogeneously dispersed NS, and strong interfacial friction.[45] In contrast to NS/PUF, the different E' values (85.1, 90.7, 79.4, and 73.5 MPa) of the PPO–NS/PUF composites with rising contents (0.5, 1, 1.5, and 2 php) are shown in Figure 9. We observed that E' of the PPO–NS/PUF composites increased greatly compared to the NS/PUF composites at lower contents (0.5 and 1 php) of filler. The remarkable improvement in E' also suggested a more favorable interfacial interaction of the PPO–NS/PUF composites compared to that of the NS/PUF composites.

The loss modulus (E'') of the NS/PUF and PPO–NS/PUF composites is shown in Figure 10. As presented in Figure 10, the E'' values of NS/PUF increased with increasing contents of NS (0, 0.5, 1, and 1.5 php) to 2 php of the NS content. The E'' value of PPO–NS/PUF was much higher compared to that of the NS/PUF composites at lower contents (0.5 and 1 php) of filler on account of the polymer grafted on the surface of the NS particles but showed no superiority at higher contents (1.5 and 2 php) of filler. That is, the polymer grafted on the NS tangled

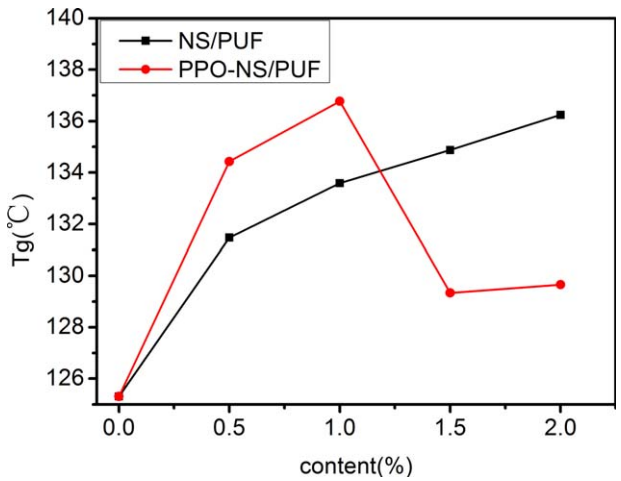

Figure 8. T_g values of the NS/PUF and PPO–NS/PUF composites with different NS contents (0, 0.5, 1, 1.5, and 2 php). [Color figure can be viewed in the online issue, which is available at wileyonlinelibrary.com.]

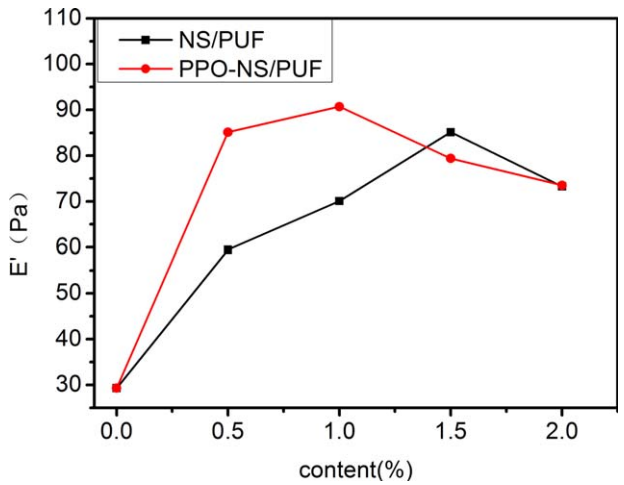

Figure 9. E' values of the NS/PUF and PPO–NS/PUF composites with different NS contents (0, 0.5, 1, 1.5, and 2 php). [Color figure can be viewed in the online issue, which is available at wileyonlinelibrary.com.]

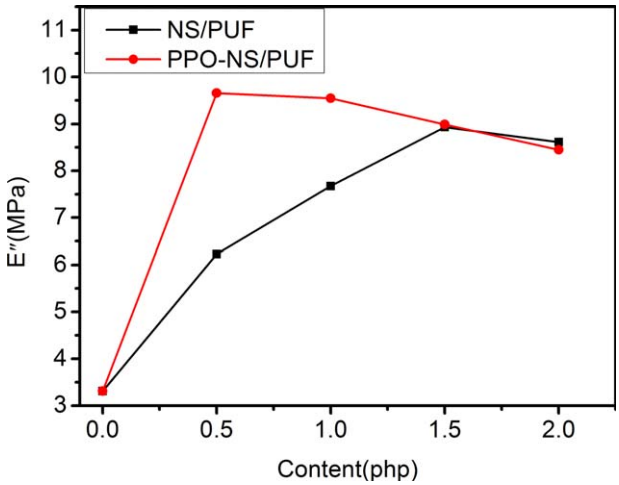

Figure 10. E'' values of the NS/PUF and PPO–NS/PUF composites with different NS contents (0, 0.5, 1, 1.5, and 2 php). [Color figure can be viewed in the online issue, which is available at wileyonlinelibrary.com.]

with the free chains of the polymer matrix and then generated greater friction when the molecular chain moved; this resulted in a higher E'' value. However, the redundant PPO–NS particles led to particle coagulation because of their numerous chain bridge effects because the same groups also existed between the PPO–NS particles and changed the particle dispersion state; this generated less friction and led to a lower E'' value.[42]

The DMA study suggested that the PUF filled with PPO–NS enjoyed favorable thermal and damping properties coupled with a high stiffness and deformation resistance because of the improved interfacial interaction between PPO–NS and the PUF matrix at lower contents of filler. This illustrated the potential applications of this material as a damping structural material.

Compression Performance of the NS/PUF Composites

As is well known, the compressive strength usually reflects the external force required to damage materials, whereas the compressive modulus reflects the ability of a material to resist deformation. The compressive properties were measured, and the specific properties (property/density) were calculated in this study to investigate the mechanical properties of the PUF composite. Generally, the mechanical reinforcement of nanocomposites can be realized if the nanoparticles are well dispersed, so the external load can be efficiently transferred via the strong interfacial interaction between the nanoparticles and the matrix. In addition, small cell size, low void fraction, and high filler loading contribute to the enhancement of the compressive properties.[44]

As revealed in Table II, the specific strength of the NS/PUF composites increased gradually from 16.87 to 18.86 MPa cm^3/g with increasing NS contents (0, 0.5, 1, and 1.5 php). However, there was a slight decrease in the specific strength of the NS/PUF composite with 2 php of the NS filler. The compressive modulus results of the NS/PUF composites were in good agreement with the specific strength data. This was attributed to the additional constraints of the nanoparticles to the segmental movement of the polymer chains, and it favored the efficient load transfer from the NS to the PUF matrix, which was provided by the interfacial interaction between NS and PU. In addition, NS served well as a heterogeneous nucleating agent during the foaming process, and this resulted in a decrease in the cell size. Therefore, in the compression process, more energy was required to destroy the composites, so the compressive strength and modulus were improved with increasing NS loadings. However, the slight decrease in the specific strength of the NS/PUF composite with 2 php of NS filler may have been caused by the uneven dispersion of NS with such an excessive loading, and this would have resulted in bigger or broken bubbles.

For the PPO–NS/PUF composites, more effective reinforcement was achieved with lower contents of filler (0.5 and 1 php) than in the NS/PUF composites. The reasons may have been as follows. The wrinkled structure of the grafted polymer on the PPO–NS surface was beneficial to its interfacial bonding with the matrix. More functional groups of the grafted polymer on the PPO–NS surface brought out stronger chemical and hydrogen-bonding interactions between PPO–NS and the PUF matrix. Thus, the interfacial interaction was more intense, and the load transfer was easier. In addition, PPO–NS acted as a more effective heterogeneous nucleating agent than NS, and this led to a decrease in the cell size. However, the mechanical reinforcement of PPO–NS at higher contents (1.5, 2 php) decreased slightly; this may have been due to the fact that the high quantity of polymer-grafted NS led to numerous chain bridges and particle coagulation.

Table II. Compressive Properties of PUFs with Different NS Contents

NS content (php)	Density (g/cm^3)	Strength (MPa)	Modulus (MPa)	Specific strength (MPa cm^3/g)
0	0.294 ± 0.004	4.96 ± 0.23	224. ± 0.7	16.87 ± 0.76
0.5 NS	0.295 ± 0.002	5.17 ± 0.11	243 ± 1.1	17.52 ± 0.37
1 NS	0.297 ± 0.002	5.50 ± 0.08	267 ± 10.7	18.51 ± 0.26
1.5 NS	0.327 ± 0.003	6.17 ± 0.01	294 ± 4.1	18.86 ± 0.03
2 NS	0.326 ± 0.002	6.13 ± 0.09	283 ± 2.8	18.80 ± 0.27
0.5 PPO-NS	0.320 ± 0.002	6.21 ± 0.11	292 ± 6.1	19.41 ± 0.34
1 PPO-NS	0.333 ± 0.002	6.21 ± 0.05	290 ± 0.6	18.65 ± 0.15
1.5 PPO-NS	0.316 ± 0.001	5.90 ± 0.04	275 ± 2.3	18.67 ± 0.13
2 PPO-NS	0.320 ± 0.002	6.01 ± 0.02	294 ± 0.2	18.78 ± 0.06

The compressive test results illustrate that PPO–NS in the PUF matrix with low contents played a vital role in the load transfer and provided more effective mechanical reinforcement.

CONCLUSIONS

In this study, PPO–NS was synthesized by an ROP catalytic process, and successful grafting was qualitatively confirmed by FTIR analysis. The grafted polymer was quantitatively characterized to be 10% by TGA, and a certain thickness of the PPO layer around each silica particle was observed directly from the TEM pictures.

The NS/PUF and PPO–NS/PUF composites were prepared by the reacting molding method to study the effect of NS and PPO–NS on the morphology and performance of PUF. In comparison with common NS particles, PPO–NS had a more significant heterogeneous nucleation effect during the foaming process of PUF; this resulted in a smaller cell size and less rupture and inhomogeneity of pores. Greater increases in T_g, E', and E'' of the PPO–NS/PUF composites were induced by the PPO–NS loading with lower filler contents (0.5 and 1 php) compared to those of the NS/PUF composites, but T_g, E', and E'' all decreased when the filler contents were further increased to 1.5 and 2 php. This was attributed to the strong interaction between the grafted polymer and the matrix, together with a steric stabilization effect of the grafted polymer. However, a high quantity of PPO–NS led to particle coagulation because of the chain bridge effect because the same groups also existed among themselves.

In addition, more effective mechanical reinforcement was achieved for the PPO–NS/PUF composites with lower contents of filler (0.5 and 1 php) than for the NS/PUF composites; this indicated that the grafted polymer on the PPO–NS surface brought out stronger chemical and hydrogen-bonding interactions between PPO–NS and the PUF matrix.

ACKNOWLEDGMENTS

The authors gratefully acknowledge the financial support of the Nature Science Foundation of China (contract grant number 51273183).

REFERENCES

1. Silva, M. C.; Takahashi, J. A.; Chaussy, D.; Belgacem, M. N.; Silva, G. G. *J. Appl. Polym. Sci.* **2010**, *117*, 3665.
2. Pan, L.-Y.; Zhan, M.-S.; Wang, K. *Polym. Eng. Sci.* **2010**, *50*, 1261.
3. Xia, H.; Song, M.; Jin, J.; Chen, L. *Macromol. Chem. Phys.* **2006**, *207*, 1945.
4. Xu, Z.; Tang, X.; Gu, A.; Fang, Z. *J. Appl. Polym. Sci.* **2007**, *106*, 439.
5. Van Hooghten, R.; Gyssels, S.; Estravis, S.; Rodriguez-Perez, M. A.; Moldenaers, P. *Eur. Polym. J.* **2014**, *60*, 135.
6. Knauert, S. T.; Douglas, J. F.; Starr, F. W. *J. Polym. Sci. Part B: Polym. Phys.* **2007**, *45*, 1882.
7. Ma, P.-C.; Siddiqui, N. A.; Marom, G.; Kim, J.-K. *Compos. Part A* **2010**, *41*, 1345.
8. Haraguchi, K.; Ebato, M.; Takehisa, T. *Adv. Mater.* **2006**, *18*, 2250.
9. Yan, D.-X.; Dai, K.; Xiang, Z.-D.; Li, Z.-M.; Ji, X.; Zhang, W.-Q. *J. Appl. Polym. Sci.* **2011**, *120*, 3014.
10. Liu, T.; Mao, L.; Liu, F.; Jiang, W.; He, Z.; Fang, P. *Wuhan Univ. J. Nat. Sci.* **2011**, *16*, 29.
11. Javni, I.; Zhang, W.; Karajkov, V.; Petrovic, Z.; Divjakovic, V. *J. Cell Plast.* **2002**, *38*, 229.
12. Nunes, R.; Fonseca, J.; Pereira, M. *Polym. Test* **2000**, *19*, 93.
13. Cho, J. W.; Lee, S. H. *Eur. Polym. J.* **2004**, *40*, 1343.
14. Yang, Z. G.; Zhao, B.; Qin, S. L.; Hu, Z. F.; Jin, Z. K.; Wang, J. H. *J. Appl. Polym. Sci.* **2004**, *92*, 1493.
15. Ahmad, S.; Ahmad, S.; Agnihotry, S. *J. Power Sources* **2005**, *140*, 151.
16. Stevenson, I.; David, L.; Gauthier, C.; Arambourg, L.; Davenas, J.; Vigier, G. *Polymer* **2001**, *42*, 9287.
17. Liu, J.; Liu, F.; Gao, K.; Wu, J.; Xue, D. *J. Mater. Chem.* **2009**, *19*, 6073.
18. Chen, G.; Zhou, S.; Gu, G.; Wu, L. *Colloid Surf. A* **2007**, *296*, 29.
19. Khan, M.; Huck, W. T. *Macromolecules* **2003**, *36*, 5088.
20. Ranjan, R.; Brittain, W. *J. Macromolecules* **2007**, *40*, 6217.
21. Rowe, M. D.; Hammer, B. A.; Boyes, S. G. *Macromolecules* **2008**, *41*, 4147.
22. Joubert, M.; Delaite, C.; Bourgeat-Lami, E.; Dumas, P. *Macromol. Rapid Commun.* **2005**, *26*, 602.
23. Joubert, M.; Delaite, C.; Bourgeat-Lami, E.; Dumas, P. *J. Polym. Sci. Part A: Polym. Chem.* **2004**, *42*, 1976.
24. Choi, I. S.; Langer, R. *Macromolecules* **2001**, *34*, 5361.
25. Cassagnau, P. *Polymer* **2008**, *49*, 2183.
26. Stober, W.; Fink, A.; Bohn, E. *J. Colloid Interface Sci.* **1968**, *26*, 62.
27. Fukushima, T.; Kosaka, A.; Yamamoto, Y.; Aimiya, T.; Notazawa, S.; Takigawa, T.; Inabe, T.; Aida, T. *Small* **2006**, *2*, 554.
28. Grunlan, J. C.; Liu, L.; Kim, Y. S. *Nano Lett.* **2006**, *6*, 911.
29. Harikrishnan, G.; Singh, S. N.; Kiesel, E.; Macosko, C. W. *Polymer* **2010**, *51*, 3349.
30. Cao, X.; James Lee, L.; Widya, T.; Macosko, C. *Polymer* **2005**, *46*, 775.
31. Chen, L.; Ozisik, R.; Schadler, L. S. *Polymer* **2010**, *51*, 2368.
32. Werner, P.; Verdejo, R.; Wöllecke, F.; Altstädt, V.; Sandler, J. K.; Shaffer, M. S. *Adv. Mater.* **2005**, *17*, 2864.
33. Yang, Y.; Gupta, M. C.; Dudley, K. L.; Lawrence, R. W. *Adv. Mater.* **2005**, *17*, 1999.
34. Thompson, M.; Motlagh, G.; Oxby, K.; Hrymak, A. *J. Appl. Polym. Sci.* **2010**, *115*, 646.
35. Song, B.; Lu, W.-Y.; Syn, C. J.; Chen, W. *J. Mater. Sci.* **2009**, *44*, 351.

36. You, M.; Zhang, X.; Wang, J.; Wang, X. *J. Mater. Sci.* **2009**, *44*, 3141.
37. Lim, H.; Kim, S. H.; Kim, B. K. *J. Appl. Polym. Sci.* **2008**, *110*, 49.
38. Kim, S. H.; Kim, B. K.; Lim, H. *Macromol. Res.* **2008**, *16*, 467.
39. Cotgreave, T.; Shortall, J. *J. Mater. Sci.* **1977**, *12*, 708.
40. Kang, M. J.; Kim, Y. H.; Park, G. P.; Han, M. S.; Kim, W. N.; Do Park, S. *J. Mater. Sci.* **2010**, *45*, 5412.
41. Verdejo, R.; Saiz-Arroyo, C.; Carretero-Gonzalez, J.; Barroso-Bujans, F.; Rodriguez-Perez, M. A.; Lopez-Manchado, M. A. *Eur. Polym. J.* **2008**, *44*, 2790.
42. Ferrero-Heredia, M.; Day, J.; Ward, W. *J. Cell Plast.* **1995**, *31*, 565.
43. Schmidt, R. H.; Kinloch, I. A.; Burgess, A. N.; Windle, A. H. *Langmuir* **2007**, *23*, 5707.
44. Lee, L. J.; Zeng, C.; Cao, X.; Han, X.; Shen, J.; Xu, G. *Compos. Sci. Technol.* **2005**, *65*, 2344.
45. Xia, H.; Song, M. *Soft Matter* **2005**, *1*, 386.